Sprouty1 has a protective role in atherogenesis and modifies the migratory and inflammatory phenotype of vascular smooth muscle cells

Xuehui Yang[1], **Chenhao Yang**[1,2], **Robert E. Friesel**[1], **Lucy Liaw**[1,2]

[1]Center for Molecular Medicine MaineHealth Institute for Research, MaineHealth Scarborough, Maine, USA 04074

[2]Graduate School of Biomedical Science and Engineering University of Maine

Abstract

Background and aims.—*Sprouty1* (*Spry1*) regulates the differentiation of vascular smooth muscle cells (VSMC), and our aim was to determine its role in atherogenesis. A significant proportion of cells within atherosclerotic lesions are derived from migration and pathological adaptation of medial VSMC.

Methods.—We used global *Spry1* null mouse, and *Myh11-Cre^ERT2, ROSA26-STOP^fl/fl-tdTomato-Spry1^fl/fl* mice to allow for lineage tracing and conditional *Spry1* deletion in VSMC. Atherosclerosis was induced by injection of a mutant form of mPCSK9$_{D377Y}$-AAV followed by Western diet. Human aortic VSMC (hVSMC) with shRNA targeting of Spry1 were also analyzed.

Results.—Global loss of *Spry1* increased inflammatory markers ICAM1 and Cox2 in VSMC. Conditional deletion of *Spry1* in VSMC had no effect on early lesion development, despite

Corresponding author: Lucy Liaw MaineHealth Institute for Research MaineHealth 81 Research Drive Scarborough, ME 04074, Lucy.Liaw@mainehealth.org.
*These authors are co-senior authors

increased Sca1^{high} cells. After 26 weeks of Western diet, mice with VSMC deletion of *Spry1* had increased plaque burden, with reduced collagen content and smooth muscle alpha actin (SMA) in the fibrous cap. Lineage tracing via tdTomato marking Cre-recombined cells indicated that VSMC with loss of *Spry1* had decreased migration into the lesion, noted by decreased proportions of tdTomato+ and tdTomato+/SMA+ cells. Loss-of-function of Spry1 in hVSMC increased mesenchymal and activation markers, including KLF4, PDGFRb, ICAM1, and Cox2. Loss of Spry1 enhanced the effects of PDGFBB and TNFa on hVSMC.

Conclusions.—Loss of *Spry1* in VSMC aggravated plaque formation at later stages, and increased markers of instability. Our results indicate that Spry1 suppresses the mesenchymal and inflammatory phenotype of VSMC, and its expression in VSMC is protective against chronic atherosclerotic disease.

Graphical Abstract
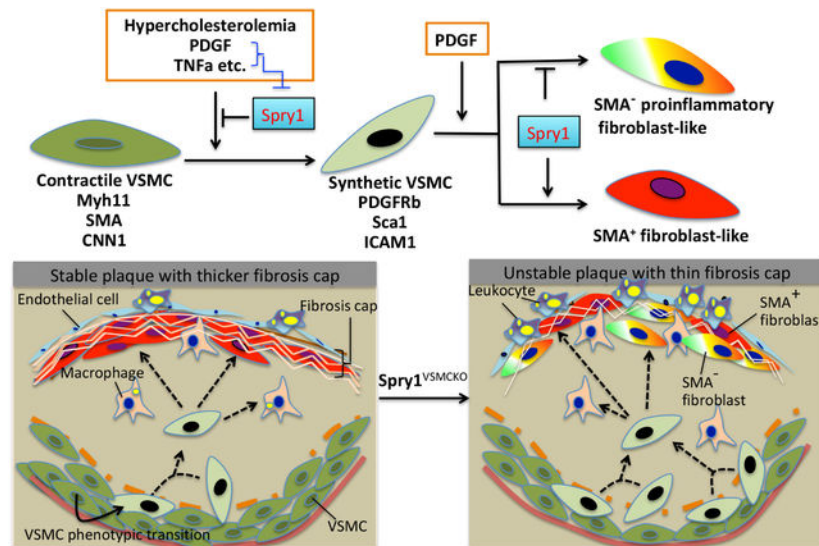
1.   Introduction

Atherosclerosis is a complex chronic inflammatory disease initiated by endothelial cell damage, leukocyte infiltration into the vessel wall, and activation and migration of vascular smooth muscle cells (VSMC) from the medial layer into the growing plaque[1–3]. Atherosclerosis in coronary arteries and resulting pathology is the leading cause of death worldwide[4]. Mortality is due to rupture of unstable atherosclerotic lesions, which can lead to thrombosis, acute myocardial infarctions, and related coronary syndromes[5,6].

VSMC have a unique ability to alter their phenotype in adaptation to cytokines or oxidative stress. As a result, they may lose their contractile characteristics and revert to mesenchymal stem cell-like, macrophage-like foam cells, or myofibroblasts[7–10]. VSMC contribute to 30%–70% of all plaque cells within an atherosclerotic lesion, and are a key determinant of the stability of advanced atherosclerotic plaques[11]. Despite many studies defining the importance and lineage of plaque cells during atherogenesis, there are still new discoveries related to upstream modifiers of VSMC that promote variant phenotypes during disease.

Sprouty1 (Spry1) is a member of the family of feedback inhibitors of receptor tyrosine kinases that are important in vascular development and diseases[12,13]. Spry1 is required to maintain the VSMC contractile phenotype *in vitro*, and plays an important role in regulation of injury-induced artery restenosis[14,15]. This study investigates the role of Spry1 in hypercholesterolemia-induced VSMC inflammatory phenotypic transition, and in the pathology of atherosclerosis.

2. Materials and methods

2.1 Mouse procedures and tissue processing.

All procedures involving animals were approved by the Maine Medical Center Institutional Animal Care and Use Committee (IACUC), and conducted in compliance with ethical and safe research practices. *Spry1LacZ* (*Spry1*$^{-/-}$) global null or wild type (*Spry1*$^{+/+}$) mice on an FVB background were from the Mouse Mutant Regional Resource Center (UC, Davis)[16]. Mice were fed a standard chow diet (2018 Teklad global 18% rodent diet, Envigo). At the time of tissue harvest, mice were euthanized with isoflurane inhalant. Aortae or carotid arteries were carefully dissected, and processed for histological analysis, RT-qPCR or immunoblotting analysis.

Spry1$^{fl/fl}$ mice, in which the *Spry1* open reading frame was flanked by loxP sequences, were on a C57BL6/J background[17]. Genotyping primers are listed in the Major Resources Table. To obtain conditional *Spry1* null mice, a *Spry1*$^{fl/fl}$ female was bred to a male *Myh11-Cre*^{ERT2} [18], and littermate breeding of *Spry1*$^{fl/+}$ with *Spry1*$^{fl/+}$;*Myh11-Cre*^{ERT2} was performed to obtain *Spry1*$^{fl/fl}$;*Myh11-Cre*^{ERT2} or *Spry1*$^{+/+}$;*Myh11-Cre*^{ERT2}. For ease of reading, we will refer to these groups as Spry1^{WT} (*Spry1*$^{+/+}$;*Myh-Cre*^{ERT2}) and Spry1^{VSMCKO} (*Spry1*$^{fl/fl}$;*Myh-Cre*^{ERT2}).

To obtain conditional *Spry1* null with simultaneous VSMC lineage-tracing, *Spry1*$^{fl/fl}$ mice were bred with *ROSA26-STOP*$^{fl/fl}$-*tdTomato* to obtain *Spry1*$^{fl/+}$;*ROSA26*+/−, and then littermate *Spry1*$^{fl/+}$;*ROSA26*+/− mice were bred to obtain *Spry1*$^{fl/fl}$;*ROSA26*$^{-/-}$ or *Spry1*$^{+/+}$;*ROSA26*$^{-/-}$. Female *Spry1*$^{fl/fl}$ were bred with male *Myh11-Cre*^{ERT2} mice to obtain *Spry1*$^{fl/+}$;*Myh-Cre*^{ERT2}, then littermates were bred to obtain *Spry1*$^{+/+}$;*Myh-Cre*^{ERT2} or *Spry1*$^{fl/fl}$;*Myh-Cre*^{ERT2}. Female *Spry1*$^{fl/fl}$;*ROSA26*$^{-/-}$ or *Spry1*$^{+/+}$;*ROSA26*$^{-/-}$ were bred with male *Spry1*$^{fl/fl}$;*Myh11-Cre*^{ERT2} or *Spry1*$^{+/+}$;*Myh11-Cre*^{ERT2}. Because the *Myh11-Cre*^{ERT2} transgene is located on the Y chromosome, all conditional null studies were performed on male mice. For ease of reading, we will refer to these groups as tdTomato-Spry1^{WT} (*Spry1*$^{+/+}$;*ROSA26*$^{-/-}$;*Myh-Cre*^{ERT2}) and tdTomato-Spry1^{VSMCKO} (*Spry1*$^{fl/fl}$;*ROSA26*$^{-/-}$;*Myh-Cre*^{ERT2}).

Cre-lox mediated recombination of *ROSA26*-tdTomato and *Spry1* deletion was induced in ~7-week-old mice after intraperitoneal injections of 1 mg of tamoxifen (T-5648, Sigma) per mouse/day for 5 days. Two days after the last tamoxifen injection, mice were injected with 10^{11} gc of adeno-associated viral vector (AAV) expressing a mutant form of murine proprotein convertase subtilisin/kexin type 9[19] (mPCSK9$_{D377Y}$-AAV, Harvard) via retroorbital injection. Mice were then fed a Western diet (D2079bi, Research Diet) containing 0.15% cholesterol for 6, 12, 18 or 26 weeks. Body weight was measured weekly.

Blood samples were collected under isofluorane anesthesia after 6 hours of fasting using hematocrit capillary tubes (22–362566, Thermofisher Scientific) for serum/plasma cholesterol measurement using a colorimetric cholesterol assay (STA-384, Cell Biolabs, Inc). On the day of harvest, mice were fasted for 6 hours and euthanized by overdose of isoflurane, and then perfused with 10 mL of PBS. Hearts, aortae, and carotid arteries were carefully dissected, fixed, and embedded in OCT or processed for further analyses.

2.2   Cell culture

Human aortic vascular smooth muscle cells (hVSMC) from at least three individual donors were obtained from Lonza or Invitrogen and cultured in SmGM2 complete medium (Lonza). Cells were used at passage 6–8 for all experiments. For knockdown studies, hVSMC were plated into 6 or 12-well plates (Falcon) at ~40% confluence and transduced with shRNA lentiviruses targeting human Spry1 or non-targeting control (NT, Open Biosystems) for ~8h, and then replaced with fresh SmGM2 medium. To test cellular responses to PDGFBB or TNFa, cells were deprived of serum and growth factors for 24h in smooth muscle cell basal medium (SmBM, Lonza), then stimulated with 20ng/ml PDGFBB or TNFa (Peprotech) for indicated time periods.

2.3   RNA sequencing.

Spry1LacZ (*Spry1$^{-/-}$*) global null or wild type (*Spry1$^{+/+}$*) mice were retroorbitally injected with 1×10^{11} gc mPCSK9$_{D377Y}$-AAV, then fed a Western diet for 4 weeks. Dorsal aortae were separated from the adventitia and used for total RNA extraction. RNA quantity and quality were assessed using the Agilent Bioanalyzer RNA 6000 Pico Chip. The RNASeq library was prepared using Stranded Illumina TruSeq, and sequenced through HiSeq Sequencing-by-Synthesis at the Vermont Integrative Genomics Resource, University of Vermont. Sequencing reads were first trimmed for quality then aligned to the most current mouse genome (mm10) using the STAR aligner. Reads were then quantified using an Expectation-Maximization model. Differential gene expression was statistically assessed and genes annotated using DESeq2 under a Negative Binomial model.

2.4   RT-PCR.

Total RNA from hVSMC or mouse arteries was extracted using RNeasy plus mini kit (Qiagen) according to the manufacturer's protocol. RNA quality and quantity were evaluated using agarose gel electrophoresis and Nanodrop spectrophotometry (Thermo Fisher), respectively. cDNA was generated using the ProtoScript First-Strand cDNA Synthesis kit (Bio-Rad), and qPCR analysis was performed using AzuraQuant Green Fast qPCR master mix (Azura). Relative mRNA levels were calculated based on the comparative Cτ (the number of amplification cycles reaching the threshold fluorescence) method using *Cypa* or *Gapdh* as internal controls. Primer sequences are listed in the Major Resources Table.

2.5   Immunoblotting.

For protein assays, cells or arteries were lysed in 2X SDS sample buffer or in HNTG buffer [50 mM HEPES, pH 7.4, 150 mM NaCl, 10% (vol/vol) glycerol, 1.5 mM MgCl$_2$, 1 mM EGTA] containing protease inhibitor cocktail (Roche), phosphatase inhibitors and

0.2% Triton X-100. Lysates were subjected to SDS-PAGE and immunoblot analysis using antibodies against ICAM-1, SPRY1, Cox2, Lrp1 (Cell Signaling Technology), SMA, and tubulin (Sigma). Antibodies are described in detail in the Major Resources Table.

2.6   Fluorescence active cell sorting (FACS).

Dorsal aortae (perivascular adipose tissue removed) from tdTomato-Spry1wt and tdTomato-Spry1[VSMCKO] mice fed a Western diet for 6 weeks were collected, digested, and processed for FACS analysis. Antibodies used were: APC/Cy7-Rat-anti-mCD68, BV421-Rat-anti-mLy6A/E(Sca1), PE-Rat-anti-mCD140b, PE-Ratanti-mCD140 from Biolegend; FITC-Rat-anti-mCD45, FITC-Rat-anti-mCD31 from BD Bioscience.

2.7   Histology and Mutiplex RNAscope analysis.

For morphological analysis, sections of aortic valves or brachiocephalic arteries were stained with hematoxylin and eosin (H&E) or Masson's trichrome stain. Immunofluorescence staining was performed by incubation with rabbit anti-CD45 (Abcam,1:100), anti-ICAM-1 (Biolegend, 1:100), anti-PDGFRb (Santa Cruz, 1:50) followed by FITC-anti-rabbit or rat IgG. FITC-anti-SMA antibody (Sigma) staining was used for tdTomato tracing immunofluorescent assays. Details of antibodies can be found in the Major Resources Table. *In situ* RNAscope assays for *Pdgfrb, Sca1, KLF4, and Spry1* were performed according to RNAscope fluorescent multiplex assay instructions (ACDBio). Images were captured using Canon EOS camera and remote imaging software (Canon), or a Leica SP8 confocal microscope. Quantification was performed using ImageJ.

2.8   Statistical analysis.

GraphPad Prism 7.0 was used to perform the statistical analyses. Data were analyzed using either 1-way or 2-way ANOVA. When justified, multiple-comparisons tests were used to determine p value. Unpaired t-tests were used for comparison of two groups of data. Differences were considered significant at $p<0.05$, and all results are reported as means ± standard deviation.

3.   Results

3.1   Global loss of Spry1 alters aortic gene expression and enhanced atherogenesis in vivo

To further our understanding of Spry1 function in VSMC physiology, we performed bulk RNA sequencing on dorsal aortae from age matched wild type ($Spry1^{+/+}$) and $Spry1$ global null ($Spry1^{-/-}$) mice (n=4 per genotype, FVB background) that were injected with mPCSK9[D377Y]-AAV and fed with Western diet for four weeks to induce hypercholesterolemia[20]. A total of 22,001 genes were sequenced. Principal Component Analysis did not show a strong change in the biological signal of aortae from $Spry1^{-/-}$ mice, likely due to a high variation within groups. However, using traditional thresholds, 276 genes passed the false discovery rate (FDR 0.2) and were significantly differentially expressed (p 0.05). The forty top differentially expressed genes are displayed in a heatmap in Supplementary Fig. 1A. Gene Ontology (GO) enrichment analysis showed the most enriched genes were associated with: 1) protein refolding (HSP90AA1, HSPA8 and

HSPH1), 2) fibroblast growth factor receptor signaling pathway (CTGF, FAT4 and FGF2), 3) glycosaminoglycan binding (SFRP1, CTGF, FGF2, ITIH4), 4) branching morphogenesis, and 5) protein kinase B activation. Heat shock proteins (HSP90AA1, HSPA8 and HSPH1) are multifunctional, and their expression is positively correlated with cardiovascular diseases[21]. Conversely, HSP90 has also been reported to bind oxidized phospholipids and prevent their further oxidation to more pathogenic and reactive products[22].

Consistent with our previous report that loss of Spry1 causes down-regulation of contractile genes in hVSMC[15], aortae from $Spry1^{-/-}$ mice had a significant reduction of calponin1 (CNN1) mRNA compared to controls by RNAseq analysis. Further, SMA immunofluorescence combined with $Spry1$ in situ RNAscope analysis showed decreased intensity of SMA protein in the $Spry1^{-/-}$ blood vessel (Supplementary Fig. 1B). Similarly decreased SMA mRNA was also observed in carotid arteries from $Spry1^{-/-}$ mice compared to wild type controls, correlating to the absence of Spry1 protein in the arteries (Supplementary Fig. 1C–D). Because of the link of inflammation to vascular disease, we analyzed several inflammatory markers including ICAM-1, which is involved in leukocyte trafficking, and Cox2, which is induced during inflammatory pathologies. We also analyzed Lrp-1, which is protective against atherosclerosis[23]. Loss of Spry1 resulted in increased levels of ICAM-1 mRNA compared to controls (Supplementary Fig. 1E). In addition, aortae from Spry1$^{-/-}$ mice had increased Cox2, but decreased Lrp-1 protein compared to controls (Supplementary Fig. 1F–G).

To determine whether these gene expression changes in $Spry1^{-/-}$ mice correlated to changes in vascular physiology, we performed an initial study of experimental atherosclerosis using age matched $Spry^{+/+}$ and $Spry1^{-/-}$ male mice (n=4/genotype). After a single injection of mPCSK9$_{D377Y}$-AAV (1×10^{11} gc/mouse), mice were fed a Western diet for 12 weeks. We found increased plaque formation in dorsal aortae and aortic valves in $Spry1^{-/-}$ mice compared to controls (Supplementary Fig. 2A–D). Immunohistochemistry to detect macrophages using F4/80 showed increased macrophage infiltration in aortic lesions from $Spry1^{-/-}$ mice (Supplementary Fig. 2E). Interestingly, one out of the four $Spry1^{-/-}$ mice had severe coronary artery plaques (Supplementary Fig. 2F), which is uncommon in atherosclerosis models in mice. The ratio of heart weight to body weight was not different based on genotype (Supplementary Fig. 2G).

3.2 Early effects of loss of Spry1 in VSMC in mice.

Mice with global loss of Spry1 on an FVB background are viable unlike the lethal phenotype on a C57BL/6 background. However, we observed multiple partially penetrant abnormalities in $Spry1^{-/-}$ mice including kidney cysts (~25–50%), enlarged uterus (>80%), and enlarged abdominal adipose tissue[24], which may contribute to atherosclerotic lesion formation. To address the role of Spry1 in VSMC in atherosclerosis more precisely, we generated tamoxifen-inducible VSMC-specific conditional $Spry1$ null mice ($Myh11$-Cre^{ERT2};$Spry1^{fl/fl}$) or control mice ($Myh11$-Cre^{ERT2};$Spry1^{+/+}$), hereafter referred to as Spry1^{VSMCKO} or Spry1^{WT} mice, respectively (Fig. 1A). Cre recombinase was induced with five consecutive tamoxifen intraperitoneal injections (1mg/mouse/day). Hypercholesterolemia was induced by a single dose of mPCSK9$_{D377Y}$-AAV (10^{11}gc/

mouse) administered via retroorbital injection. Mice were fed a high fat, Western diet. Atherosclerosis is a heterogeneous process in humans; similarly, we observed heterogeneous plaque formation in the aortae in mice. At 12 weeks after Western diet feeding, there were no significant differences in aortic plaque area (Fig. 1B–C), and total serum cholesterol levels (Fig. 1D) and body weight were similar between groups. We also analyzed lesions along the aortic root (Fig. 1E), and assessed lipid accumulation and plaque size using oil Red O staining (Fig. 1F). The lesion area in aortic valves in Spry1^{VSMCKO} mice showed a trend towards smaller plaques compared to those in Spry1^{WT} mice (Fig. 1F–G).

Changes in VSMC induced by hypercholesterolemia include increased Sca1 and PDGFRb expression[10,25]. Thus, we performed *in situ* multiplex RNAScope analysis to examine expression of *Sca1*, *PDGFRb* and *Spry1* mRNA. *Spry1* mRNA in wild type mice was detected in aortic VSMC, adventitial cells, and some plaque cells, and was specifically deleted in VSMC in aortic arteries in Spry1^{VSMCKO} mice (Fig. 1H, K). *Sca1* positive cells were observed in the medial VSMC in lesions from both genotypes and in non-lesion areas in *Spry1^{VSMCKO}* mice (Fig. 1I, L). It is worth stressing that *Sca1* positive cells were distributed in a scattered pattern, particularly in medial layers of the aortae. Nonetheless, Spry1^{VSMCKO} mice had significantly elevated *Sca1* positive cells in plaques compared to controls (Fig. 1K–L) whereas there were no differences in the aortic media. The mRNA of *KLF4*, another key regulator of VSMC mesenchymal transition, was also increased in aortic sections from Spry1^{VSMCKO} mice (Supplementary Fig. 3A). FACS analysis on aortic cells also suggested a trend of increased Sca1+, CD61 and CD140a+ cell populations in Spry1^{VSMCKO} mice compared to Spry1^{WT} mice, although this did not reach statistical significance (Supplementary Fig. 3B). We also assessed *PDGFRb* mRNA expression in aortic valve medial layer cells compared to controls (Fig. 1H, J, K, and M), and levels between groups were similar.

3.3   Spry1 deficiency reduces CD45+ cell infiltration and VSMC migration into the plaque.

The migration of VSMC from the media to the intima plays an important role in plaque formation. To better quantify VSMC populations and trace the movement of medial VSMC, we generated tamoxifen-inducible VSMC-specific conditional Spry1 null mice with simultaneous VSMC lineage-tracing in *Myh11-Cre^{ERT2}ROSA26-STOP$^{fl/fl}$-tdTomatoSpry1$^{fl/fl}$* or *Spry1$^{+/+}$* mice, hereafter referred as tdTomato-Spry1^{VSMCKO} or tdTomato-Spry1^{WT} mice, respectively. These double transgenic mice were treated with tamoxifen to induce Cre, followed by a single injection of mPCSK9$_{D377Y}$-AAV and 6 weeks of Western diet (Fig. 2A). Upon tissue harvest, the adipose tissue was removed from the aorta, and vessel wall cells were dissociated by collagenase digestion and subjected to flow cytometry to analyze the proportions of tdTomato, Sca1 and PDGFRb-producing cells. We observed that loss of Spry1 in VSMC decreased overall tdTomato positive cells, while the proportion of Sca1+ and PDGFRb/Sca1 double positive cells did not change (Fig. 2B).

Next, we used Bodipy™493/503, a tracer for neutral lipids, to visualize the localization of lipids in VSMC and atherosclerotic lesions. Hypercholesterolemia induces heterogeneous lesion formation with various degrees of tdTomato+ VSMC involvement (Fig. 2C). While the overall tdTomato positive cells in the plaques in aortic roots was not different between

genotypes (Fig. 2D), it is worth noting that we observed a dim tdTomato signal in plaques from tdTomato-Spry1^{VSMCKO} mice (Fig. 2C and 2F), indicating loss of *Spry1* in VSMC may alter tdTomato protein metabolism. The dim tdTomato positive cells likely were excluded in FACS analysis, resulting in overall decreased tdTomato+ cells in tdTomato-Spry1^{VSMCKO} mice (Fig. 2B), a discrepancy compared to data from cell counting results (Fig. 2D and Fig. 2G). We also quantified the location of these cells in the plaque with relation to the internal elastic lamina (dotted line) to assess distance of VSMC migration. There were more Spry1^{VSMCKO} tdTomato positive cells closer to the internal elastic lamina (Fig. 2E), within 10μm from the internal elastic lamina. In addition, tdTomato cells from Spry1^{WT} mice were throughout the plaque, including >70μm away from the internal elastic lamina, which was not seen in plaques from Spry1^{VSMCKO} mice. There was ~1.8 fold decrease in the total distance of tdTomato positive cells from the internal elastic lamina in the aortic root lesions of Spry1^{VSMCKO} mice compared to Spry1^{WT}mice.

We used the same analysis in the aortae (Fig. 2F–H). Similarly, the overall number of tdTomato positive cells within plaques did not vary by genotype (Fig. 2G). However, like in the aortic roots, we found increased tdTomato positive cells closer to the internal elastic lamina (within 5μm) in the lesions of Spry1^{VSMCKO} mice compared to Spry1^{WT} mice (Fig. 2H). Additionally tdTomato positive cells from Spry1^{WT} mice were found >50μm from the internal elastic lamina, whereas this was not observed in the plaques of Spry1^{VSMCKO} mice. In the plaques of the aortae, there was ~1.9 fold decrease in total distance of tdTomato positive cells from the internal elastic lamina in the lesions of Spry1^{VSMCKO} mice compared to Spry1^{WT} mice. These results are consistent with our previous report that loss of Spry1 decreased hVSMC migration *in vitro*[15].

Endothelial damage and leukocyte infiltration is an important component of lesion formation with hypercholesterolemia. We performed immunofluorescence staining to detect leukocytes with the pan-leukocyte marker CD45 (Fig. 2I). In the aortic root plaques after nine weeks of high fat diet, overall lesion size did not differ based on genotype (Fig. 2J). However, the number of CD45 positive cells / plaque area was significantly decreased in lesions from Spry1^{VSMCKO} mice compared to Spry1^{WT} mice (Fig. 2K).

3.4   Spry1 deficiency in VSMC leads to increased advanced plaque burden and decreased indices of plaque stability under prolonged hypercholesterolemia

Given the chronic nature of atherosclerosis, which develops over decades in humans, we were interested whether *Spry1* deficiency has effect on lesion formation and stability with long-term hypercholesterolemia. Using the same mouse models, we performed a study to extend high fat diet feeding for 26 weeks, until the mice were 34 weeks of age (Fig. 3A). Analysis was performed in the aortic roots, the brachiocephalic arteries, and the aortae (Fig. 3B). There were no differences in plasma cholesterol between the genotypes (Fig. 3C). In contrast to shorter term high fat diet feeding, after 26 weeks, Spry1^{VSMCKO} mice had increased plaque formation visualized by whole mount Sudan IV staining on *en face* dorsal aortae (Fig. 3D–E). Serum cholesterol is a known risk factor, and levels in the mouse after high fat feeding were variable between individuals. Thus, we performed correlation analysis on cholesterol level vs. aortic lesion area. The plaque area positively correlated with

cholesterol levels in Spry1^{WT} mice, but not in Spry1^{VSMCKO} mice (Fig. 3F), indicating the increased plaque burden with loss of Spry1 protein in VSMC is independent of cholesterol level.

Next, we examined the morphology of plaques by H&E staining. Brachiocephalic arteries and aortic roots from mice of both genotypes formed complex lesions with an imperfectly formed fibrous cap overlying a central necrotic, lipid-laden plaque (Fig. 3G, 3J). Loss of Spry1 in VSMC had no effect on atherosclerotic lesion size in the brachiocephalic arteries (Fig. 3G) or overall necrotic area (Fig. 3H). However, because of the high variability in size of lesions and necrotic area/plaque, we quantified the proportion of necrosis within each plaque. Plaques from Spry1^{VSMCKO} mice had a higher proportion of necrotic area per plaque compared to those from Spry1^{WT} mice (Fig. 3I). In the aortic roots (Fig. 3J), loss of Spry1 in VSMC led to increased plaque area (Fig. 3K), but no changes in overall necrotic area or proportion of necrosis within each plaque (Fig. 3L).

The level of collagen deposition in lesion is a useful indicator of plaque stability. Using Masson's Trichrome stain, we observed non-uniform fibrosis caps, with some overlaid by a layer of xanthoma, particularly in Spry1^{VSMCKO} plaques (Fig. 4A–B). Loss of Spry1 in VSMC decreased overall collagen content in lesions within the brachiocephalic arteries (Fig. 4A) and aortic roots (Fig. 4B). VSMC migration to the fibrous cap and re-expression of genes associated with VSMC differentiation, such as SMA, contribute to plaque stability. We therefore examined the tdTomato+ VSMC localization in cap areas as well as SMA protein localization. Using immunofluorescence and confocal microscopy, we observed thicker SMA-stained fibrous caps in both the brachiocephalic artery (Fig. 4C) and aortic root lesions (Fig. 4D) in Spry1^{WT} compared to Spry1^{VSMCKO} mice. The SMA positive fibrous caps were contiguous along the lumenal border of the plaque in Spry1^{WT} mice, whereas the staining in plaques from Spry1^{VSMCKO} mice was discontinuous with less SMA staining (white arrows).

We then assessed the tdTomato+ cell localization within the subendothelial fibrotic cap of coronary cusps of aortic valves (Fig. 4E–G). In lesions from Spry1^{VSMCKO} mice, we observed decreased proportions of tdTomato+ cells and tdTomato+, SMA+ double positive cells (Fig. 4E–F). Conversely, loss of Spry1 in VSMC resulted in increased proportions of non-tdTomato positive cells (negative) in subendothelial cap regions (Fig. 4G). In addition, CD45+ leukocyte infiltration into the subendothelial compartment was significantly increased in plaques from Spry1^{VSMCKO} mice compared to those from Spry1^{WT} mice (Fig. 4H–I, and Fig. S4A–B). Our results indicate that endogenous Spry1 functions in the pathogenesis of atherosclerosis include promotion of VSMC migration throughout the lesion, particularly to the fibrous cap, where it promotes SMA expression and stabilization of the plaque. This is associated with enhanced collagen deposition within the lesion. Loss of *Spry1* in VSMC impairs the differentiated phenotype of fibrous cap cells and leads to increased leukocyte accumulation in the subendothelial region of the lesion.

3.5 Deleting Spry1 in human VSMC in vitro increases mesenchymal and inflammatory marker expression

To determine whether the loss of function phenotype of Spry1 in VSMC in mice correlated to its activity in human VSMC, we studied human VSMC *in vitro*. Spry1 is expressed in human VSMC, and we utilized shRNA lentivirus targeting Spry1 for loss-of-function studies. Consistent with our previous report[15], suppression of Spry1 promoted a synthetic phenotype in human VSMC with lower levels of the contractile marker calponin and increased levels of the mesenchymal markers *KLF4* and *PDGFRb* (Fig. 5A). Inflammatory activation of medial VSMC correlates to formation of atherosclerotic plaques. Suppression of Spry1 increased *ICAM-1*, a molecule involved in leukocyte trafficking and inflammation pathology, and *CCL2*, a chemokine, while not affecting *SDF-1* transcript level. Immunoblotting confirmed higher ICAM-1 protein in VSMC with Spry1 knockdown (Fig. 5B–C).

PDGFB/PDGFR signaling induces VSMC cytokine expression and inflammation[7]. We tested whether increased PDGFRb expression in Spry1 knockdown human VSMC affects downstream signaling and altered cytokine expression. PDGFBB stimulation increased *CCL2* and *CCL3* mRNA, suppression of Spry1 did not alter induction of *CCL2*, but reduced induction of *CCL3* transcript (Fig. 5D). Spry1 mRNA was transiently decreased by PDGFBB stimulation at 2 hr, and restored thereafter (Fig. 5D). PAI-1 is another critical factor that contributes to the pathogenesis of cardiovascular diseases[26]. We found that basal mRNA level of *PAI-1* in human VSMC was elevated after suppression of Spry1, with the same effect after PDGFBB stimulation (Fig. 5E). In addition, the increased basal ICAM-1 protein in Spry1 knockdown human VSMC was further increased by PDGFBB stimulation (Fig. 5F–G). We also observed that suppression of Spry1 increased Cox2 protein. PDGFBB stimulation decreased Cox2 protein in control cells, and to a less degree in Spry1 knockdown human VSMC (Fig. 5F–G). Interestingly, PDGFBB stimulation markedly decreased Spry1 protein levels, and this effect was sustained up to 24 hours, unlike the transient decrease in *Spry1* mRNA (Fig. 5D).

Next, we examined human VSMC response to TNFa. Consistent with its pro-inflammatory activity, TNFa markedly increased the mRNA expression of cytokines and factors including *CCL2*, *IL-6*, and *PAI-1* in human VSMC. Conversely, TNFa stimulation significantly decreased Spry1 mRNA (Fig. 5H) and protein (Fig 5I–J). The elevated Cox2 protein in Spry1 knockdown human VSMC was further increased by TNFa stimulation (Fig. 5I, K).

4.   Discussion

The regulation of the pro-inflammatory phenotype of VSMC in atherosclerotic lesion progression and stability is complex and multi-factorial. In this study, we investigated the effects of Spry1 production in VSMC, and consequences of its loss-of-function in atherogenesis. We used a mouse model targeting Spry1 in VSMC using inducible *Myh11*Cre[ERT2], and also used a Cre-activated tdTomato lineage tracing method to track the fate of VSMC in the atherosclerotic plaque. Our studies represent the first description of Spry1 function in the vasculature during vascular obstructive disease. We showed that hypercholesterolemia caused a small set of VSMC to convert to a *Sca1^{high}* mesenchymal

stem-like cell, and *Spry1* deficiency enhanced this effect. Loss of Spry1 in VSMC resulted in increased CD45+ cell infiltration into the subendothelial plaque layer, and advanced plaque burden and instability after prolonged high fat diet. In addition, *Spry1* deficient VSMC had compromised restoration of SMA expression in the fibrous cap of advanced lesions. These studies in the mouse were correlated to loss-of-function studies using human VSMC. *In vitro* suppression of Spry1 in VSMC increased the expression of ICAM-1, Cox2, PAI1, and PDGFRb inflammatory mesenchymal markers, and promoted, to some extent, PDGFBB or TNFa-induced inflammatory effects. Together, our findings indicate that endogenous Spry1 suppresses the transition of VSMC into a proinflammatory mesenchymal transition, and promotes migration and differentiation of fibrous cap VSMC, suggesting that Spry1 plays a protective role in atherosclerosis. Despite lesion size not changing with the absence of Spry1 in our mouse model of atherogenesis, mortality in human disease is not correlated with plaque size, but rather plaque rupture due to instability[27–29]. Thus, Spry1 action to promote fibrous cap formation and collagen deposition is predicted to increase plaque stability.

Atherosclerosis is a chronic, progressive condition with a long asymptomatic phase. Most plaques remain subclinical, and vulnerable atherosclerotic plaques containing a thin inflamed fibrous cap over a large lipid core are particularly susceptible to disruption[27,30]. VSMC investment into and retention within the lesion and fibrous cap contributes to stabilization of atherosclerotic plaques. PDGF/PDGFRb signaling not only drives VSMC to a secretory phenotype, synergizes with hypercholesterolemia to promote the formation of advance atherosclerotic plaques, but also is essential for VSMC investment and transition to a SMA+ myofibroblast-like state[31]. PDGFRb signaling-induced aerobic glycolysis in VSMC allows robust extracellular matrix deposition and SMA synthesis to stabilize advanced plaques [11,31]. Our current results show that Spry1 deficiency increased PDGFRb expression, and to some extent synergized with PDGF- and TNFa-mediated VSMC inflammation, suggesting a negative role for Spry1 on PDGF and TNFa-initiated VSMC inflammation. Interestingly, PDGFBB and TNFa markedly suppressed Spry1 protein expression in VSMC. We previously reported that Spry1 is a key molecule to maintain VSMC in a contractile phenotype[15]. Therefore, VSMC-specific deletion of Spry1 may mediate, at least in part, some effects mediated by PDGF and TNFa signaling. However, VSMC-specific *Spry1* deletion resulted in a compromised restoration of SMA expression in the fibrous cap. This and other decreased stability indices in advanced plaques indicates that Spry1 has a role in maintaining fibrous cap stability independent of PDGFR signaling.

Spry1 mRNA was only transiently down-regulated at 2 hrs following PDGF stimulation, and thereafter was restored in VSMC *in vitro*. The different dynamics of steady state transcripts versus protein is common in mammalian cells. Therefore, it is possible that *Spry1* mRNA transcription and later translation is necessary for PDGF/PDGFRb signaling mediated SMA expression in cap VSMC. The gap between Spry1 protein down-regulation and restoration maybe also necessary to ensure PDGF-induced VSMC mesenchymal transition. Indeed, we have reported that growth factor enriched medium (SmGM2) transient down-regulates Spry1 protein in hVSMC *in vitro*[14]. Further investigation is needed to address the role of the dynamic expression of Spry1 protein downstream of PDGF/PDGFRb signaling. Currently,

there is no available anti-SPRY1 specific antibody for immunofluoresence staining that could allow for more focused study of SPRY1 protein dynamics in VSMC.

Cellular clonal expansion contributing to human atherosclerotic lesions was first identified by Benditt et al[32]. The concept of VSMC monoclonality in atherosclerotic lesions was consolidated using X-linked inactivation assays and polymerase chain reaction techniques[33,34]. Recently, use of multicolor reporter mice demonstrated that VSMCs in murine plaques are derived by the clonal expansion of a very few cells in the medial arterial wall[25,35–38]. The hypercholesterolemia-induced appearance of scattered *Sca1^{high}* VSMC within the media in wild type mice may also be due to expansion and migration of clonal VSMC that contribute to the atherogenic lesion. *Spry1* deficiency increased *Sca1^{high}* cells in the medial layer of vessels, indicating that loss of Spry1 may increase conversion of VSMC into atherogenic prone cells or clonal cell expansion of plaque cells.

The remodeling and turnover of VSMC, which is achieved through processes such as selective cell proliferation/apoptosis or matrix synthesis/degradation, is very low in a normal adult artery[39,40]. Unlike the ubiquitously expressed SPRY1 protein that we previously detected by immunohistochemistry[14] (production of Spry1 antibody used in the previous study was discontinued), the scattered *Spry1* mRNA expression in the normal medial layer may result from low VSMC remodeling and turnover. Similarly, we observed a steady high tdTomato in the normal medial layer and a decreased/punctuated tdTomato signal in VSMC next to the atherosclerotic lesion, suggesting that loss of *Spry1* increases VSMC remodeling and turnover.

VSMC-specific *Spry1* deletion resulted in reduced fatty streak formation during early atherosclerosis despite an increased inflammatory phenotypic transition of VSMC. Atherosclerosis is a progressive process, in which endothelial cell dysfunction induced by oxidative stress initiates leukocyte infiltration and following fatty streak formation[41–43]. High cholesterol is a critical risk factor in atherosclerosis[44,45]. A single intravenous PCSK9DY-AAV injection followed by western diet feeding is an effective and relatively rapid approach that doesn't require multiple genetic mutations for atherogenesis; this model results in rapid and long-term sustained hyperlipidemia and atherosclerosis[19]. Using this method, we consistently generated hypercholesterolemia and atherogenesis. We observed slightly lower serum cholesterol levels in VSMC-specific *Spry1* null mice compared to controls, without noticeable differences in food consumption or body weight gain. It is possible that loss of Spry1 in VSMC affects lipid metabolism, and future studies will address this possibility. Also in VSMC-specific *Spry1* null mice, there was less CD45+ cell infiltration and smaller fatty streak formation compared to controls. In summary, our findings indicate that endogenous Spry1 suppresses the mesenchymal-like transition of VSMC, and thus is protective in chronic atherosclerotic disease.

Supplementary Material

Refer to Web version on PubMed Central for supplementary material.

Acknowledgements

References

1. Libby P, Ridker PM, Hansson GK. Progress and challenges in translating the biology of atherosclerosis. Nature. 2011;473:317–325. doi: 10.1038/nature10146 [PubMed: 21593864]

2. Soehnlein O, Libby P. Targeting inflammation in atherosclerosis - from experimental insights to the clinic. Nat Rev Drug Discov. 2021;20:589–610. doi: 10.1038/s41573-021-00198-1 [PubMed: 33976384]

3. Crowther MA. Pathogenesis of atherosclerosis. Hematology Am Soc Hematol Educ Program. 2005:436–441. doi: 10.1182/asheducation-2005.1.436 [PubMed: 16304416]

4. Tsao CW, Aday AW, Almarzooq ZI, Alonso A, Beaton AZ, Bittencourt MS, Boehme AK, Buxton AE, Carson AP, Commodore-Mensah Y, et al. Heart Disease and Stroke Statistics-2022 Update: A Report From the American Heart Association. Circulation. 2022;145:e153–e639. doi: 10.1161/cir.0000000000001052 [PubMed: 35078371]

5. Weber C, Noels H. Atherosclerosis: current pathogenesis and therapeutic options. Nat Med. 2011;17:1410–1422. doi: 10.1038/nm.2538 [PubMed: 22064431]

6. Rosenfeld ME, Campbell LA. Pathogens and atherosclerosis: update on the potential contribution of multiple infectious organisms to the pathogenesis of atherosclerosis. Thromb Haemost. 2011;106:858–867. doi: 10.1160/TH11-06-0392 [PubMed: 22012133]

7. He C, Medley SC, Hu T, Hinsdale ME, Lupu F, Virmani R, Olson LE. PDGFRbeta signalling regulates local inflammation and synergizes with hypercholesterolaemia to promote atherosclerosis. Nat Commun. 2015;6:7770. doi: 10.1038/ncomms8770 [PubMed: 26183159]

8. Bennett MR, Sinha S, Owens GK. Vascular Smooth Muscle Cells in Atherosclerosis. Circ Res. 2016;118:692–702. doi: 10.1161/CIRCRESAHA.115.306361 [PubMed: 26892967]

9. Gomez D, Owens GK. Smooth muscle cell phenotypic switching in atherosclerosis. Cardiovasc Res. 2012;95:156–164. doi: 10.1093/cvr/cvs115 [PubMed: 22406749]

10. Yap C, Mieremet A, de Vries CJM, Micha D, de Waard V. Six Shades of Vascular Smooth Muscle Cells Illuminated by KLF4 (Kruppel-Like Factor 4). Arterioscler Thromb Vasc Biol. 2021;41:2693–2707. doi: 10.1161/ATVBAHA.121.316600 [PubMed: 34470477]

11. Shankman LS, Gomez D, Cherepanova OA, Salmon M, Alencar GF, Haskins RM, Swiatlowska P, Newman AA, Greene ES, Straub AC, et al. KLF4-dependent phenotypic modulation of smooth muscle cells has a key role in atherosclerotic plaque pathogenesis. Nat Med. 2015;21:628–637. doi: 10.1038/nm.3866 [PubMed: 25985364]

12. Lee S, Bui Nguyen TM, Kovalenko D, Adhikari N, Grindle S, Polster SP, Friesel R, Ramakrishnan S, Hall JL. Sprouty1 inhibits angiogenesis in association with up-regulation of p21 and p27. Mol Cell Biochem. 2010;338:255–261. doi: 10.1007/s11010-009-0359-z [PubMed: 20054616]

13. Yang X, Gong Y, Friesel R. Spry1 is expressed in hemangioblasts and negatively regulates primitive hematopoiesis and endothelial cell function. PLoS One. 2011;6:e18374. doi: 10.1371/journal.pone.0018374 [PubMed: 21483770]

14. Yang X, Gong Y, He Q, Licht JD, Liaw L, Friesel RE. Loss of Spry1 attenuates vascular smooth muscle proliferation by impairing mitogen-mediated changes in cell cycle regulatory circuits. J Cell Biochem. 2018;119:3267–3279. doi: 10.1002/jcb.26486 [PubMed: 29105817]

15. Yang X, Gong Y, Tang Y, Li H, He Q, Gower L, Liaw L, Friesel RE. Spry1 and Spry4 differentially regulate human aortic smooth muscle cell phenotype via Akt/FoxO/myocardin signaling. PLoS One. 2013;8:e58746. doi: 10.1371/journal.pone.0058746 [PubMed: 23554919]

16. Thum T, Gross C, Fiedler J, Fischer T, Kissler S, Bussen M, Galuppo P, Just S, Rottbauer W, Frantz S, et al. MicroRNA-21 contributes to myocardial disease by stimulating MAP kinase signalling in fibroblasts. Nature. 2008;456:980–984. doi: 10.1038/nature07511 [PubMed: 19043405]

17. Basson MA, Akbulut S, Watson-Johnson J, Simon R, Carroll TJ, Shakya R, Gross I, Martin GR, Lufkin T, McMahon AP, et al. Sprouty1 is a critical regulator of GDNF/RET-mediated kidney induction. Dev Cell. 2005;8:229–239. doi: 10.1016/j.devcel.2004.12.004 [PubMed: 15691764]

18. Wirth A, Benyo Z, Lukasova M, Leutgeb B, Wettschureck N, Gorbey S, Orsy P, Horvath B, Maser-Gluth C, Greiner E, et al. G12-G13-LARG-mediated signaling in vascular smooth muscle is required for salt-induced hypertension. Nat Med. 2008;14:64–68. doi: nm1666 [pii] 10.1038/ nm1666 [PubMed: 18084302]

19. Roche-Molina M, Sanz-Rosa D, Cruz FM, Garcia-Prieto J, Lopez S, Abia R, Muriana FJ, Fuster V, Ibanez B, Bernal JA. Induction of sustained hypercholesterolemia by single adeno-associated virus-mediated gene transfer of mutant hPCSK9. Arterioscler Thromb Vasc Biol. 2015;35:50–59. doi: 10.1161/ATVBAHA.114.303617 [PubMed: 25341796]

20. Jarrett KE, Lee C, De Giorgi M, Hurley A, Gillard BK, Doerfler AM, Li A, Pownall HJ, Bao G, Lagor WR. Somatic Editing of Ldlr With Adeno-Associated Viral-CRISPR Is an Efficient Tool for Atherosclerosis Research. Arterioscler Thromb Vasc Biol. 2018;38:1997–2006. doi: 10.1161/ ATVBAHA.118.311221 [PubMed: 30026278]

21. Rodriguez-Iturbe B, Johnson RJ. Heat shock proteins and cardiovascular disease. Physiol Int. 2018;105:19–37. doi: 10.1556/2060.105.2018.1.4 [PubMed: 29602292]

22. Zhang M, Wang D, Xu X, Xu W. Evaluation of antioxidant property of heat shock protein 90 from duck muscle. Anim Biosci. 2021;34:724–733. doi: 10.5713/ajas.19.0854 [PubMed: 32777911]

23. Overton CD, Yancey PG, Major AS, Linton MF, Fazio S. Deletion of macrophage LDL receptor-related protein increases atherogenesis in the mouse. Circ Res. 2007;100:670–677. doi: 10.1161/01.RES.0000260204.40510.aa [PubMed: 17303763]

24. Yang X, Pande S, Koza RA, Friesel R. Sprouty1 regulates gonadal white adipose tissue growth through a PDGFRalpha/beta-Akt pathway. Adipocyte. 2021;10:574–586. doi: 10.1080/21623945.2021.1987634 [PubMed: 34714716]

25. Dobnikar L, Taylor AL, Chappell J, Oldach P, Harman JL, Oerton E, Dzierzak E, Bennett MR, Spivakov M, Jorgensen HF. Disease-relevant transcriptional signatures identified in individual smooth muscle cells from healthy mouse vessels. Nat Commun. 2018;9:4567. doi: 10.1038/ s41467-018-06891-x [PubMed: 30385745]

26. Ji Y, Weng Z, Fish P, Goyal N, Luo M, Myears SP, Strawn TL, Chandrasekar B, Wu J, Fay WP. Pharmacological Targeting of Plasminogen Activator Inhibitor-1 Decreases Vascular Smooth Muscle Cell Migration and Neointima Formation. Arterioscler Thromb Vasc Biol. 2016;36:2167– 2175. doi: 10.1161/ATVBAHA.116.308344 [PubMed: 27659097]

27. Bentzon JF, Otsuka F, Virmani R, Falk E. Mechanisms of plaque formation and rupture. Circ Res. 2014;114:1852–1866. doi: 10.1161/circresaha.114.302721 [PubMed: 24902970]

28. Fuster V, Stein B, Ambrose JA, Badimon L, Badimon JJ, Chesebro JH. Atherosclerotic plaque rupture and thrombosis. Evolving concepts. Circulation. 1990;82:II47–59. [PubMed: 2203564]

29. Newby AC, Libby P, van der Wal AC. Plaque instability--the real challenge for atherosclerosis research in the next decade? Cardiovasc Res. 1999;41:321–322. [PubMed: 10341831]

30. Rosenfeld ME, Averill MM, Bennett BJ, Schwartz SM. Progression and disruption of advanced atherosclerotic plaques in murine models. Curr Drug Targets. 2008;9:210–216. doi: 10.2174/138945008783755575 [PubMed: 18336239]

31. Newman AAC, Serbulea V, Baylis RA, Shankman LS, Bradley X, Alencar GF, Owsiany K, Deaton RA, Karnewar S, Shamsuzzaman S, et al. Multiple cell types contribute to the atherosclerotic lesion fibrous cap by PDGFRbeta and bioenergetic mechanisms. Nat Metab. 2021;3:166–181. doi: 10.1038/s42255-020-00338-8 [PubMed: 33619382]

32. Benditt EP, Benditt JM. Evidence for a monoclonal origin of human atherosclerotic plaques. Proc Natl Acad Sci U S A. 1973;70:1753–1756. doi: 10.1073/pnas.70.6.1753 [PubMed: 4515934]

33. Murry CE, Gipaya CT, Bartosek T, Benditt EP, Schwartz SM. Monoclonality of smooth muscle cells in human atherosclerosis. Am J Pathol. 1997;151:697–705. [PubMed: 9284818]

34. Chung IM, Schwartz SM, Murry CE. Clonal architecture of normal and atherosclerotic aorta: implications for atherogenesis and vascular development. Am J Pathol. 1998;152:913–923. [PubMed: 9546352]

35. Misra A, Feng Z, Chandran RR, Kabir I, Rotllan N, Aryal B, Sheikh AQ, Ding L, Qin L, Fernandez-Hernando C, et al. Integrin beta3 regulates clonality and fate of smooth muscle-derived atherosclerotic plaque cells. Nat Commun. 2018;9:2073. doi: 10.1038/s41467-018-04447-7 [PubMed: 29802249]

36. Chappell J, Harman JL, Narasimhan VM, Yu H, Foote K, Simons BD, Bennett MR, Jorgensen HF. Extensive Proliferation of a Subset of Differentiated, yet Plastic, Medial Vascular Smooth Muscle Cells Contributes to Neointimal Formation in Mouse Injury and Atherosclerosis Models. Circ Res. 2016;119:1313–1323. doi: 10.1161/CIRCRESAHA.116.309799 [PubMed: 27682618]

37. Jacobsen K, Lund MB, Shim J, Gunnersen S, Füchtbauer EM, Kjolby M, Carramolino L, Bentzon JF. Diverse cellular architecture of atherosclerotic plaque derives from clonal expansion of a few medial SMCs. JCI Insight. 2017;2. doi: 10.1172/jci.insight.95890

38. Wang Y, Nanda V, Direnzo D, Ye J, Xiao S, Kojima Y, Howe KL, Jarr KU, Flores AM, Tsantilas P, et al. Clonally expanding smooth muscle cells promote atherosclerosis by escaping efferocytosis and activating the complement cascade. Proc Natl Acad Sci U S A. 2020;117:15818–15826. doi: 10.1073/pnas.2006348117 [PubMed: 32541024]

39. Gordon D, Reidy MA, Benditt EP, Schwartz SM. Cell proliferation in human coronary arteries. Proc Natl Acad Sci U S A. 1990;87:4600–4604. doi: 10.1073/pnas.87.12.4600 [PubMed: 1972277]

40. McCarthy NJ, Bennett MR. The regulation of vascular smooth muscle cell apoptosis. Cardiovasc Res. 2000;45:747–755. doi: 10.1016/s0008-6363(99)00275-8 [PubMed: 10728397]

41. Gimbrone MA Jr., Garcia-Cardena G Endothelial Cell Dysfunction and the Pathobiology of Atherosclerosis. Circ Res. 2016;118:620–636. doi: 10.1161/CIRCRESAHA.115.306301 [PubMed: 26892962]

42. Howe KL, Fish JE. Transforming endothelial cells in atherosclerosis. Nat Metab. 2019;1:856–857. doi: 10.1038/s42255-019-0100-5 [PubMed: 32694742]

43. Davignon J, Ganz P. Role of endothelial dysfunction in atherosclerosis. Circulation. 2004;109:III27–32. doi: 10.1161/01.CIR.0000131515.03336.f8 [PubMed: 15198963]

44. Rosenbaum MA, Miyazaki K, Graham LM. Hypercholesterolemia and oxidative stress inhibit endothelial cell healing after arterial injury. J Vasc Surg. 2012;55:489–496. doi: 10.1016/j.jvs.2011.07.081 [PubMed: 22047834]

45. Hong Z, Staiculescu MC, Hampel P, Levitan I, Forgacs G. How cholesterol regulates endothelial biomechanics. Front Physiol. 2012;3:426. doi: 10.3389/fphys.2012.00426 [PubMed: 23162471]

Highlights

- Global deletion of Spry1 promoted atherogenesis.

- Conditional deletion of Spry1 using Myh11-Cre[ERT2] increased *Sca1* and *PDGFRb* mRNA expression in plaques, reduced leukocyte infiltration, and reduced VSMC migration into the intima.

- In advanced atherosclerotic lesions, loss of Spry1 in VSMC increased plaque burden, decreased collagen deposition, and decreased markers of plaque stability.

- Knockdown of Spry1 using lentivirus shRNA increased the expression of pro-inflammatory ICAM1, Cox2 and PAI1, and mesenchymal markers KLF4 and PDGFRb in human VSMC *in vitro*.
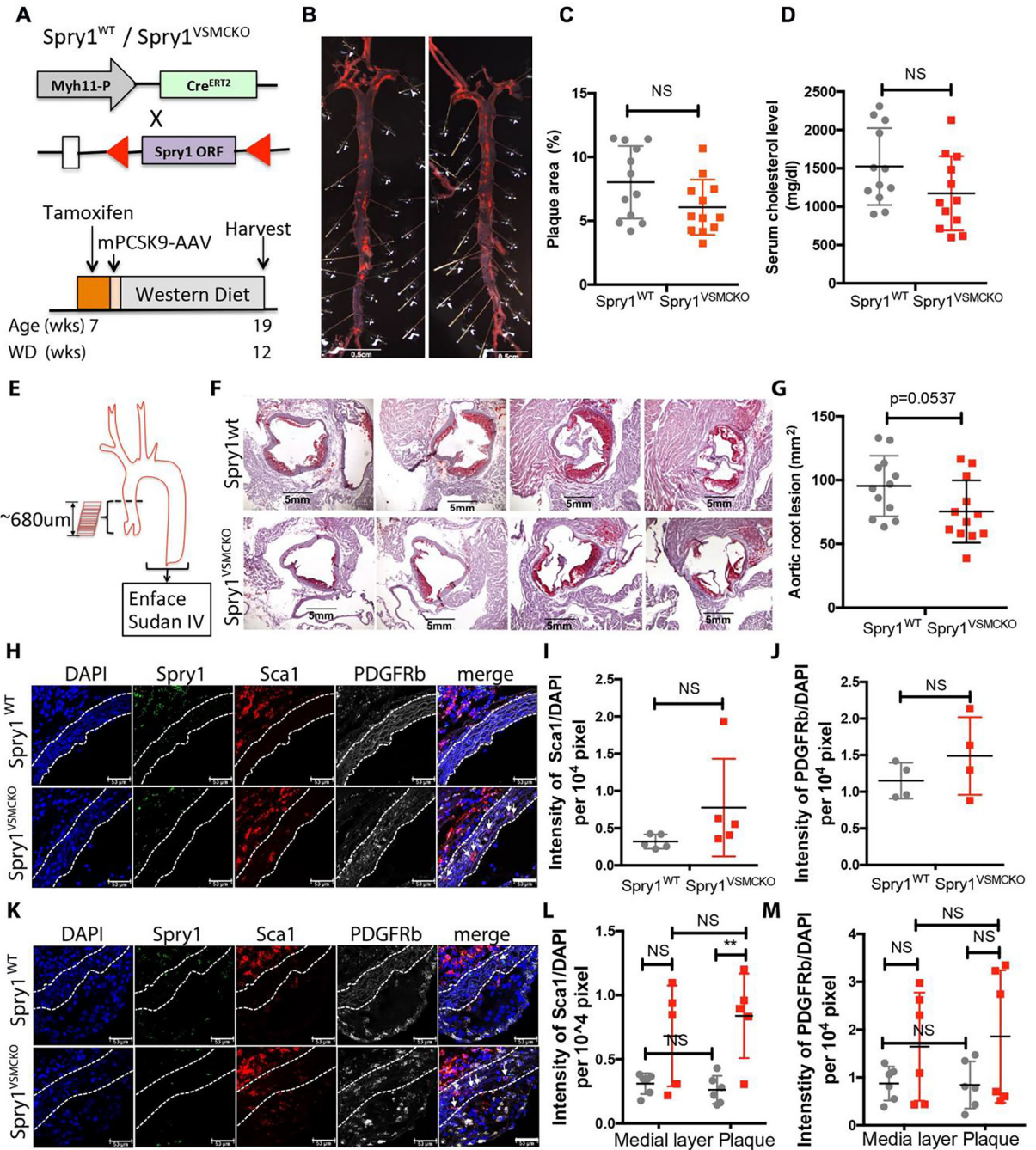
Figure 1.
Loss of Spry1 does not affect overall atherosclerotic plaque, but increases Sca1+ cells in lesions. (A) Overview of mouse model and experimental design. Spry1^WT and Spry1^VSMCKO mice received tamoxifen injections at 7 weeks of age, followed by one mPCSK9$_{D377Y}$-AAV retroorbital injection (10^{11}gc/mouse), and western diet (WD) feeding for 12 wks. (B) *En face* Sudan IV staining of lipid species in aortae was used as a measure of plaque area, which is quantified in (C). (D) Mouse serum was collected after fasting for 6 hours at the end of the experiment for quantification of total cholesterol. (E) Schematic of the aortic root

region for sectioning and histologic analysis. (F) Representative oil Red O stained images from four sequential segments (~170μm per segment) of aortic roots. Staining is quantified in (G). (H) Representative images of multicolor RNAScope analysis of Spry1, Sca1 (white arrows), and PDGFRb mRNA in aortic roots regions without plaque, with quantification of these areas outside of the lesion in (I-J). (K) Representative images of multicolor RNAScope analysis of Spry1, Sca1 (white arrows), and PDGFRb mRNA in aortic root plaques, with quantification in (L-M). Graphs show means ± SD and p values were determined using either a 2-way ANOVA with alpha=0.05 followed by multiple comparisons test (L-M), or t-test (C, D, G, I-J). **p<0.01
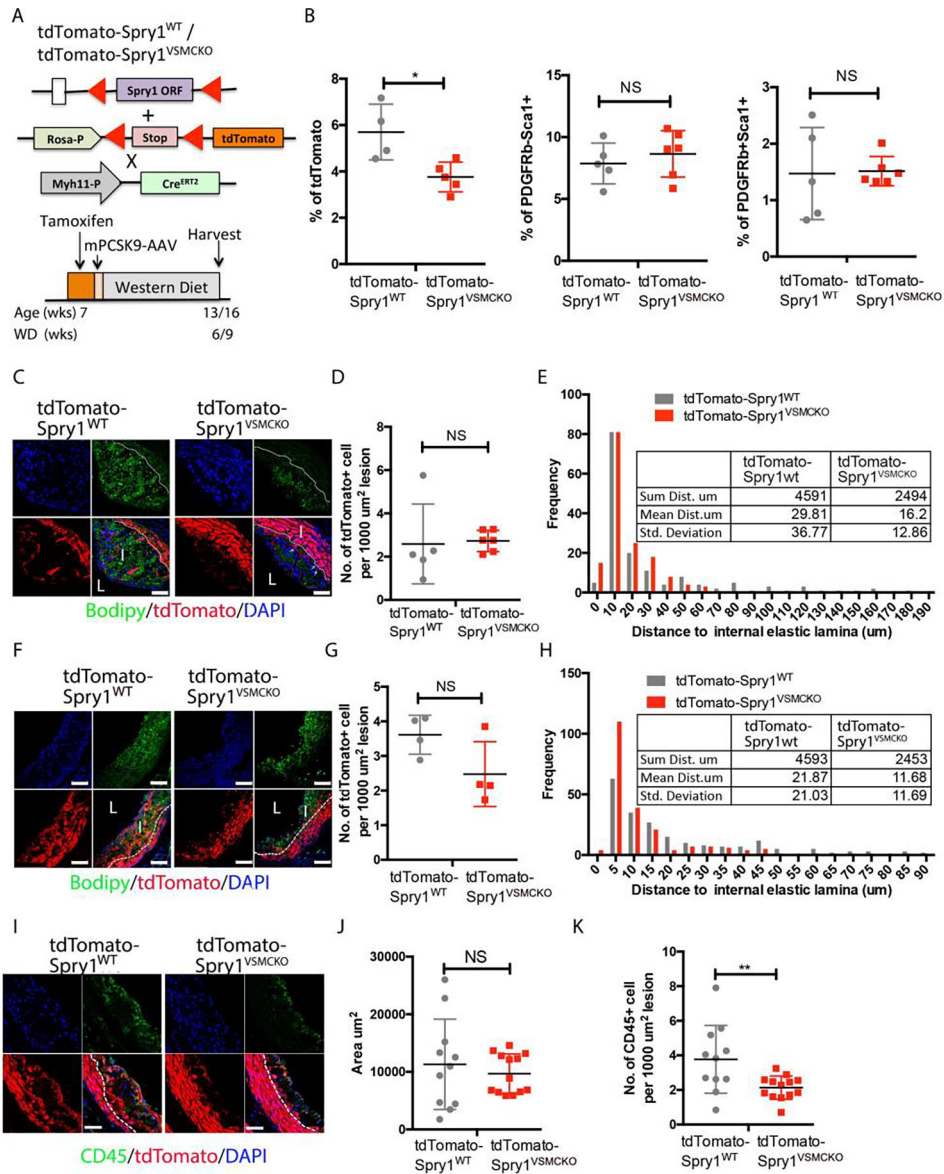
Figure 2.
Loss of Spry1 alters migration pattern of VSMC and reduces CD45+ cells in plaques.
(A) Schematic of the mouse model and experimental design. *Myh11-CreERT2;tdTomato-ROSA26-STOP^{fl/fl}-Spry1^{fl/fl}* or Spry1^{WT} mice received 5 intraperitoneal (IP) tamoxifen injections in corn oil at 7 weeks of age to label smooth muscle cells with tdTomato (tdTomato-Spry1^{VSMCKO} or tdTomato-Spry1^{WT}, respectively). Mice received a single mPCSK9-AAV retroorbital injection (10^{11}gc/mouse), followed by Western diet (WD) feeding for 6 or 9 weeks before analysis. (B) After 6 weeks of Western diet, dorsal aortae were processed (n=6) for FACS analysis, and the proportion of tdTomato+, Sca1+, and PDGFRb+ cells quantified. (C) Aortic root sections were stained with Bodipy™493/503 to visualize lipids. Representative confocal images show lipids (green) and tdTomato+ cells (red). Scar bar = 50μm. (D) Quantification of tdTomato+ cells within lesions (n=6/genotype). (E) The distance of tdTomato+ cells to the inner elastic lamina (white dashed

line) was measured using Image J. The frequency distribution of 154 measurements / genotype was analyzed in Prism. (F) Sections from the aortae after 9 weeks of Western diet were stained by Bodipy™493/503 to visualize lipids (green), scar bar = 60μm. (G) Quantification of tdTomato+ cells / plaque area (n=4 / genotype). (H) Distribution of tdTomato+ cell distances from 210 measurements / genotype. (I) CD45 staining was used to quantify leukocytes. Scar bar = 50μm. (J) Plaque area was calculated, and used to normalize number of CD45+ cells / genotype (K). Graphed are means ± SD, p values were determined using t-test. *p<0.05; **p<0.01.
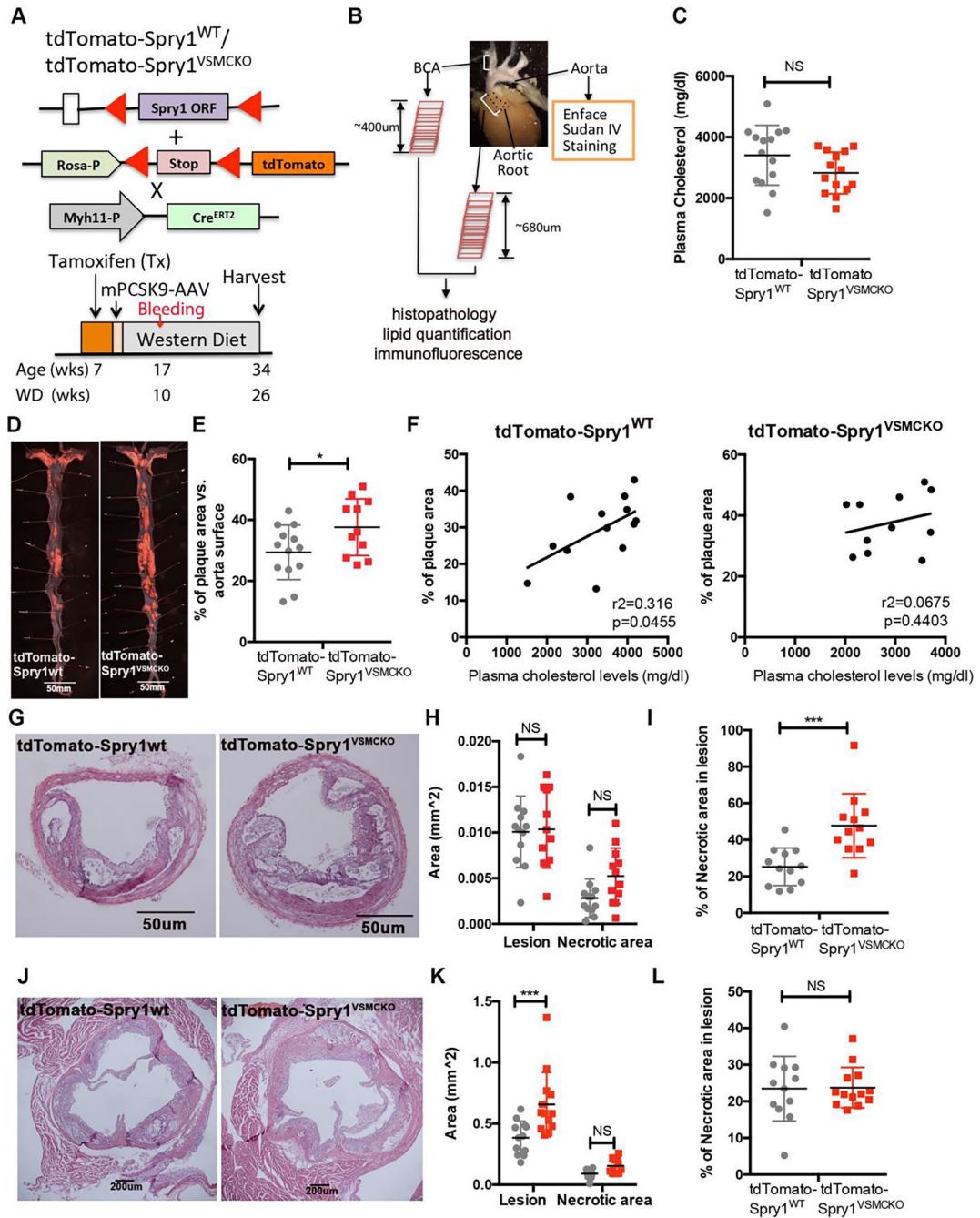
Figure 3.
Spry1 deficiency in VSMC leads to increased advanced plaque burden and necrosis. (A and B) Schematic of the mouse model, experimental design and analysis. (C) Six-hour fasting plasma was collected after Western diet (WD) feeding for 10 weeks (n=12/group). (D) Representative images of aorta *en face* Sudan IV staining, and quantification of lipid area (E). Spry1[VSMCKO] mice had more lipid deposition in aortae compared to controls. (F) Correlation of lipid area with plasma cholesterol levels. Sections from three sequential segments (one section per segment) of brachiocephalic arteries (G, ~130μm per segment) or

aortic roots (J, ~220μm per segment) were stained with H&E. Average areas of plaques and necrotic cores were quantified from three sections from each group from brachiocephalic arteries (H-I) or aortic roots (K-L). Graphed are means ± SD, p values were determined using either 2-way ANOVA with alpha=0.05 followed by multiple comparisons test (H, K), or t-test (C, E, F, I, and L). *p<0.05; **p<0.01; ***p<0.001; n=12 for each genotype).
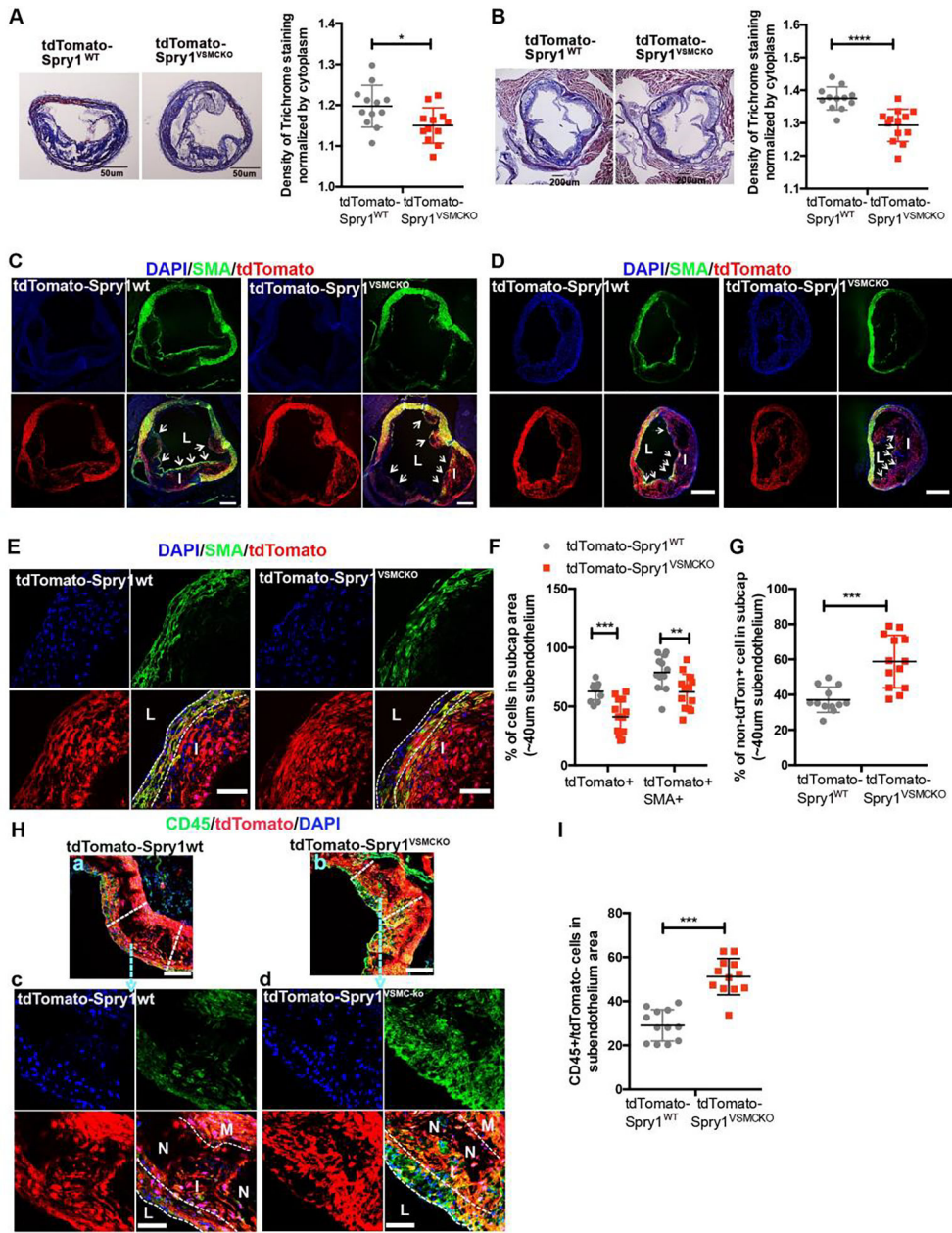
Figure 4.

Loss of Spry1 in VSMC leads to decreased indices of advanced plaque stability. Masson's Trichrome stain of brachiocephalic arteries (A) or aortic roots (B) with quantification of trichrome stain from three sequential segments. Plaque collagen content was quantified by measuring blue collagen intensity, and then normalized to pink cytoplasm intensity. Immunofluorescence staining using FITC-conjugated mouse monoclonal anti-SMA (green) to examine SMA expression in brachiocephalic arteries (C) or aortic roots, scar bar = 200um. (D) to visualize the fibrous cap. Scale bar = 230μm. White arrows show SMA-positive fibrous cap regions. (E) Representative images of left coronary cusp lesion cap areas in aortic roots. Double broken white lines indicate a ~40μm subendothelial fibrotic

cap region. L=lumen, I = intima. Scale bar = 63μm. (F) TdTomato+ and SMA+ cells in this area were quantitated from three segments. (G) The proportion of tdTomato negative cells was compared between genotypes. (H) Representative images from aortic roots stained to detect CD45 (green). Lower magnification images were represented in a and b, scar bar = 120um. Areas within the double dash lines were imaged at higher magnification, and represented in c and d, respectively. Scar bar = 50um. The subendothelial region is indicated by dashed lines. L=lumen, I = intima, M=media, and N=necrotic area. Scale bar = 50μm. (I) The proportion of CD45 positive cells was quantified. Average CD45+tdTomato- cells were calculated from three segments. Graphed are means ± SD, p values were determined using either 2-way ANOVA with alpha=0.05 followed by multiple comparisons test (F, G), or t-test (B). *p<0.05; **p<0.01; ***p<0.001; n=12 for each genotype.
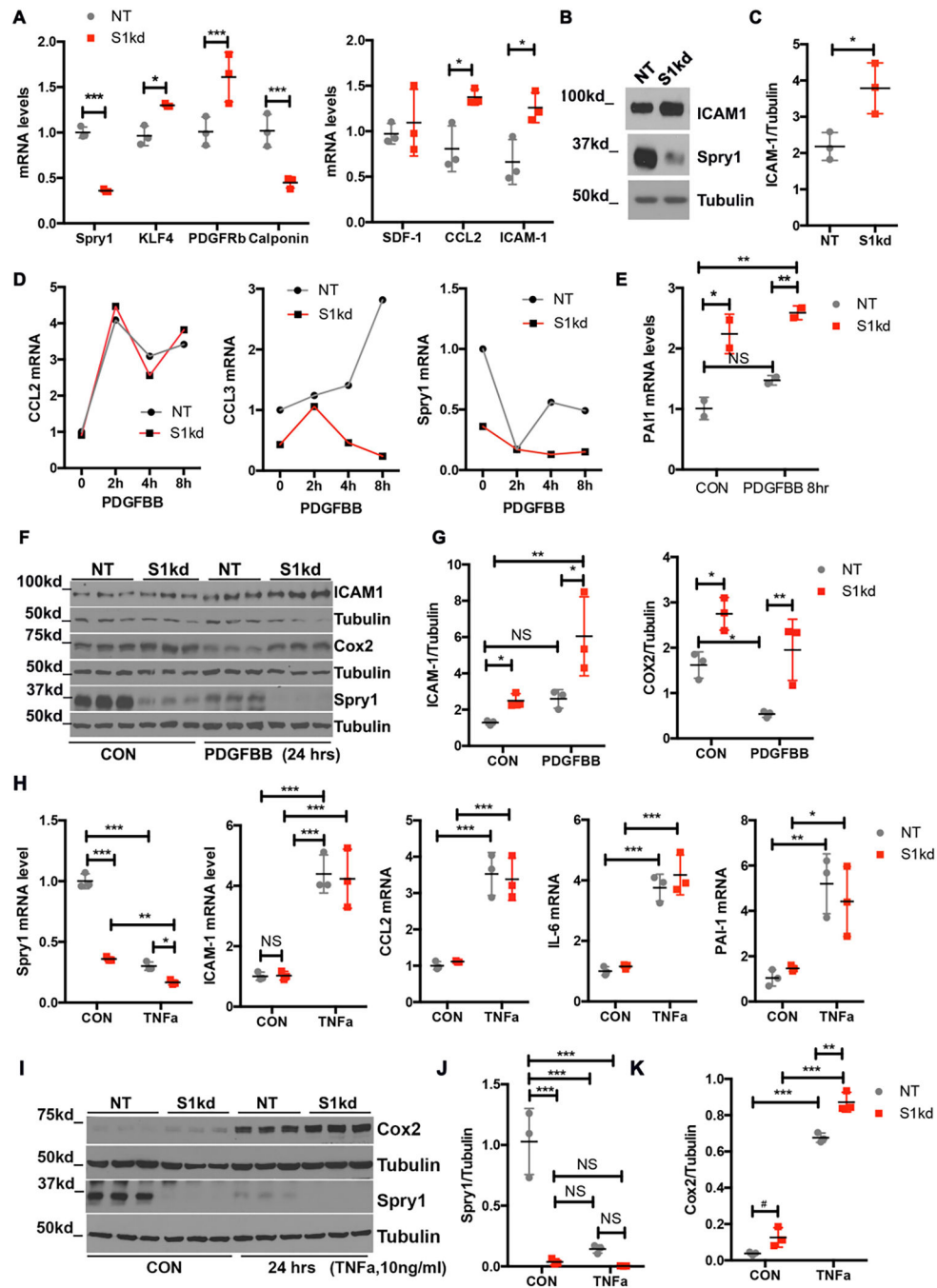
Figure 5.
Deletion of Spry1 in hVSMC regulates mesenchymal and inflammatory markers.
(A) Spry1 shRNA lentivirus was used to reduce Spry1 protein in human VSMC (S1kd).
Cells were used for RT-qPCR analysis in triplicate to quantify transcripts for calponin,
KLF4 and PDGFRb, CCL2, and ICAM-1. (B) Representative immunoblotting of ICAM-1
and C) quantification from three independent experiments. (D) Cells were made quiescent
in basal SBM2 medium, and analyzed after PDGFBB (20ng/ml) stimulation. (E) RT-qPCR
analysis for PAI-1 mRNA after PDGFBB stimulation for 8 hrs. (F) Human VSMC were

serum starved for 24h, then stimulated with PDGFBB for 24 hrs, and lysates collected for immunoblotting to quantify ICAM-1, Cox2, Spry1 and Tubulin. (G) ICAM-1 and Cox2 protein levels were quantified using ImageJ. (H) Cells were treated with 10ng/ml TNFa for 24 hrs, and subjected for RT-qPCR analysis to evaluate Spry1, ICAM-1, CCL2, IL-6, and PAI-1 mRNA expression. (I) Cell lysates were immunoblotted to quantify Spry1 (J) and Cox2 (K) protein. mRNA or protein values are graphed as means ± SD. p values were determined using either a 2-way ANOVA with alpha=0.05 followed by multiple comparisons test (A, E, G, H, J), or t-test (C). *p<0.05; **p<0.01; ***p<0.001.